Sci Eng Compos Mater 19 (2012): 323–330 © 2012 by Walter de Gruyter • Berlin • Boston. DOI 10.1515/secm-2012-0011

# The effects of cutouts on buckling behavior of composite plates

**Ahmet Erkliğ* and Eyüp Yeter**

Engineering Faculty, Mechanical Engineering Department, University of Gaziantep, Gaziantep, Turkey,
e-mail: erklig@gantep.edu.tr

*Corresponding author

## Abstract

Cutouts such as circular, rectangular, square, elliptical, and triangular shapes are generally used in composite plates as access ports for mechanical and electrical systems, for damage inspection, to serve as doors and windows, and sometimes to reduce the overall weight of the structure. This paper addresses the effects of different cutouts on the buckling behavior of plates made of polymer matrix composites. To study the effects of cutouts on buckling, loaded edges are taken as fixed and unloaded edges are taken as free. Finite element analysis is also performed to predict the effects of different geometrical cutouts, orientations, and position of cutouts on the buckling behavior. The results show that fiber orientation angle and cutout sizes are the most important parameters on the buckling loads. For all types of cutouts the buckling loads decrease dramatically by increasing the fiber orientation angle. It is observed that minimum buckling load is reached when 45° fiber angle is used, and after this angle critical buckling load begins to increase. Also, it is concluded that while fiber orientation angle is 0°, elliptical cutout has the highest buckling load and while fiber orientation angle is 45°, circular cutout has the highest buckling load.

**Keywords:** buckling; composite plates; cutouts; finite element.

## 1. Introduction

Composite material is a structural material consisting of two or more combined constituents that are combined at a macroscopic level and are not soluble in each other [1]. Composite materials have been increasingly used in aircraft and space vehicle structures as plates and shells because of their comparatively high strength-to-weight and stiffness-to-weight ratios. They are used in the following industries: automotive, construction, marine, corrosion resistant equipment, consumer products and appliance/business equipment.

Composite plates are used extensively in the form of relatively thin plate, and consequently the load-carrying capability of composite plate against buckling is very important and has been intensively considered by researchers. Also, composite plates are often provided with cutouts as design requirements. Therefore, the correct understanding of buckling characteristics of composite plates with cutouts is necessary. Buckling analysis of plates with different cutout shapes has been studied by many researchers. In early studies, Lin and Kuo [2] examined buckling of symmetrically or anti-symmetrically laminated composite plates with circular holes under in-plane static loadings. Nemeth [3] presented a study on buckling behavior of rectangular symmetric angle-ply plates with a central circular cutouts for loaded and unloaded edges clamped and simply supported, respectively. An approximate analysis for buckling of biaxial- and shear-loaded anisotropic panels with centrally located elliptical cutouts was presented by Britt [4]. Lee and Hyer [5] studied the failure mechanisms found in a plate with a centrally located circular hole loaded in-plane into the post-buckling range of deflections.

Akbulut and Sayman [6] recently conducted a buckling analysis of rectangular composite plates with a central square hole. The critical loads of symmetric angle-ply, anti-symmetric cross-ply or angle-ply laminates were found for constant or various thicknesses, simple or clamped boundary conditions, simple or biaxial loading *versus* hole sizes. Ghannadpour et al. [7] investigated the effect of a circular cutout on the buckling behavior of rectangular symmetric cross-ply laminates. Baltacı et al. [8] investigated buckling analysis of laminated composite circular plates having circular holes and subjected to uniform radial load by using the finite element method. Mechanical buckling behaviors of composite square plates of four symmetric and anti-symmetric layers with circular holes were examined by Yapıcı et al. [9]. Baba and Baltaci [10] investigated the effects of anti-symmetric laminate configuration, cutout and length/thickness ratio on the buckling behavior of E/glass-epoxy composite plates. Akbulut and Ural [11] studied the buckling behaviors of simply supported composite laminated square plates with corner circular notches under in-plane static loadings. Yazıcı [12] studied the influence of square cutout on the buckling stability of multilayered, steel-woven fiber-reinforced polypropylene thermoplastic matrix composite plates by using numerical and experimental methods. A numerical and experimental study was carried out to determine the effect of circular hole diameter and location on the buckling behavior of woven fabric E-glass/epoxy composite plates by Sahin [13]. Topal and Uzman [14] studied the design of simply supported symmetrically laminated composite plates with central circular holes. Qablan et al. [15] evaluated the effect of various parameters on the buckling load of square cross-ply laminated plates with circular cutouts. Buckling analysis of a woven-glass-polyester laminated composite plate with a circular/elliptical hole was carried out by Komur et al. [16].

From the above-mentioned literature, buckling analysis of composite plates with different cutout shapes such as circular holes [2, 3, 7–9, 11, 13–16], elliptical holes [4, 16] square or rectangular holes [6, 12] has been the subject of many researches. Results presented in the related literature indicate that the buckling behavior of composite plates is affected by cutout shape, cutout size and cutout orientation. However, the combination of variables considered during previous studies is still limited. Parameters that affect the critical buckling load, such as cutout shape, were examined separately in previous studies. In this study, effects of different cutout shapes (circular, triangular, square and elliptical), cutout sizes and cutout orientations on the buckling behavior of composite plates are taken into consideration. Different plate sizes, fiber orientation angles and stacking sequences are also examined.

## 2. Materials and methods

### 2.1. Material properties

In this study, laminated glass-polyester composite plates are produced and mechanical properties obtained from experiments are used in the finite element analyses and in the theoretical calculations. The composite plies are laid up to form eight-ply laminates having $[\theta]_8$ stacking sequences. Fiber orientations in the ply were taken as 0°, 15°, 30°, 45° and 60°. Effect of size of plates and cutouts orientation angles are investigated by using five different plate sizes (100, 150, 200, 250 and 300 mm) and four different cutout orientation angles (0°, 15°, 30°, 45°). The mechanical properties of the glass-polyester composite material are listed in Table 1.

### 2.2. Theoretical formulation of buckling loads

For the case of mid-plane symmetry, it is seen that buckling is a non-linear effect. The in-plane strains are given by the following formula, where it is seen that the next (non-linear) term in the McLauren series has been included [17]:

$$\varepsilon_x=\frac{\partial u}{\partial x}+\frac{1}{2}\left(\frac{\partial w}{\partial x}\right)^2;\ \varepsilon_y=\frac{\partial v}{\partial y}+\frac{1}{2}\left(\frac{\partial w}{\partial y}\right)^2;$$
$$\varepsilon_{xy}=\frac{\gamma_{xy}}{2}=\frac{1}{2}\left(\frac{\partial u}{\partial y}+\frac{\partial v}{\partial x}+\frac{\partial w}{\partial x}\frac{\partial w}{\partial y}\right) \tag{1}$$

The results including the terms to predict the advent or inception of buckling for the plate are given in the following equation, which is for a specific orthotropic plate, modified to include buckling effects:

$$D_1\frac{\partial^4 w}{\partial x^4}+2D_3\frac{\partial^4 w}{\partial x^2\partial y^2}+D_2\frac{\partial^4 w}{\partial y^4}=p(x,y)$$
$$+N_x\frac{\partial^2 w}{\partial x^2}+2N_{xy}\frac{\partial^2 w}{\partial x\,\partial y}+N_y\frac{\partial^2 w}{\partial y^2} \tag{2}$$

It is clearly seen that there is a coupling between the in-plane loads and the lateral deflection. However, in actual structural analysis, the effect of lateral loads, along with the in-plane loads, could cause overstress and failure before the buckling load is reached. Looking now at Eq. (2) for the buckling of the composite plate under an axial load per unit width only, and ignoring $p(x,y)$, Eq. (2) becomes:

$$D_1\frac{\partial^4 w}{\partial x^4}+2D_3\frac{\partial^4 w}{\partial x^2\partial y^2}+D_2\frac{\partial^4 w}{\partial y^4}-N_x\frac{\partial^2 w}{\partial x^2}=0 \tag{3}$$

For the case of the plate simply supported on all four edges, one assumes the Navier solution:

$$w(x,y)=\sum_{m=1}^{\infty}\sum_{n=1}^{\infty}A_{mn}\sin\frac{m\pi x}{a}\sin\frac{n\pi y}{b} \tag{4}$$

Substituting Eq. (4) into Eq. (3), we get critical load as in the Eq. 5:

$$P_{cr}=N_{xcr}=-\frac{\pi^2a^2}{m^2}\left[D_1\left(\frac{m}{a}\right)^4+2D_3\left(\frac{m}{a}\right)^2\left(\frac{n}{b}\right)^2+D_2\left(\frac{n}{b}\right)^4\right] \tag{5}$$

where

$$D_1=D_{11},\ D_2=D_{22},\ D_3=D_{12}+2D_{66} \tag{6}$$

Putting Eq. (6) to Eq. (5), one gets the Eq. (7) as:

$$P_{cr}=\pi^2\left[D_{11}\left(\frac{m}{a}\right)^2+2\left(D_{12}+2D_{66}\right)\left(\frac{n}{b}\right)^2+D_{22}\left(\frac{n}{b}\right)^4\left(\frac{m}{a}\right)^2\right] \tag{7}$$

At this point, several things become clear: Eq. (7) is a homogeneous equation. However, it is not clear which value of $m$ and $n$ results in the lowest critical buckling load. All values of $n$ appear in the numerator, so $n$=2 is the necessary value for this case of loaded edges are fixed and unloaded edges are free. But $m$ appears in several places, and depending on the value of the flexural stiffness $D_{11}$, $D_{12}$, $D_{22}$ and $D_{66}$ and the length-to-width ratio of the plate, $a/b$, it is not clear which value of $m$ will provide the lowest value; however, for a given plate it can easily be determined computationally.

Then taking $n$=2, Eq. (7) becomes:

$$P_{cr}=\pi^2\left[D_{11}\left(\frac{m}{a}\right)^2+2\left(D_{12}+2D_{66}\right)\left(\frac{2}{b}\right)^2+D_{22}\left(\frac{2}{b}\right)^4\left(\frac{m}{a}\right)^2\right] \tag{8}$$

where $D_{11}$, $D_{12}$, $D_{22}$ and $D_{66}$ are components of bending stiffness matrices $[D]$ and calculated by using Eq. (9) as:

$$D_{ij}=\frac{1}{3}\sum_{k=1}^{n}\left[\bar{Q}_{ij}\right]_k\left(h_k^3-h_{k-1}^3\right),\ i=1,2,6;\ j=1,2,6; \tag{9}$$

**Table 1** Material properties.

| $E_1=E_2$ (GPa) | $G_{12}$ (GPa) | $\upsilon_{12}$ |
|---|---|---|
| 31.610 | 3.220 | 0.206 |

$h$ values are shown in Figure 1. The formulas are:

$$h=\sum_{k=1}^{n} t_k;\ h_0=-\frac{h}{2}(top\ surface);$$
$$h_1=-\frac{h}{2}+t_1(top\ surface);\ h_2=-\frac{h}{2}+t_2;\ldots \tag{10}$$

$$h_{k-1}=-\frac{h}{2}+\sum_{1}^{k-1} t\ (top\ surface);$$
$$h_k=-\frac{h}{2}+\sum_{=1}^{k} t\ (bottom\ surface);\ k=2,3,\ldots,\ n\text{-}2,\ n\text{-}1 \tag{11}$$

Then to find the reduced stiffness matrix [$Q$] for each ply, Eq. (12) is used.

$$Q_{11}=\frac{E_1}{1-\upsilon_{21}\upsilon_{12}};\ Q_{12}=\frac{\upsilon_{12}E_2}{1-\upsilon_{21}\upsilon_{12}};$$
$$Q_{22}=\frac{E_2}{1-\upsilon_{21}\upsilon_{12}};\ Q_{66}=G_{12} \tag{12}$$

Finally, to calculate the transformed stiffness matrix $\left[\overline{Q}\right]$ of Eq. (9), the following equations are used:

$$\begin{aligned}
\overline{Q}_{11}&=Q_{11}\cos^4\theta+Q_{22}\sin^4\theta+2\left(Q_{12}+2Q_{66}\right)\sin^2\theta\cos^2\theta\\
\overline{Q}_{12}&=(Q_{11}+Q_{22}-4Q_{66})\sin^2\theta\cos^2\theta+Q_{12}\left(\cos^4\theta+\sin^2\theta\right)\\
\overline{Q}_{22}&=Q_{11}\sin^4\theta+Q_{22}\cos^4\theta+2\left(Q_{12}+2Q_{66}\right)\sin^2\theta\cos^2\theta\\
\overline{Q}_{16}&=(Q_{11}-\theta_{12}-2Q_{66})\sin\theta\cos^3\theta-(Q_{22}-Q_{12}-2Q_{66})\sin^3\theta\cos\theta\\
\overline{Q}_{26}&=(Q_{11}-\theta_{12}-2Q_{66})\sin^3\theta\cos\theta-(Q_{22}-Q_{12}-2Q_{66})\sin\theta\cos^3\theta\\
\overline{Q}_{66}&=(Q_{11}+Q_{22}-2Q_{12}-2Q_{66})\sin^2\theta\cos^2\theta+Q_{66}(\sin^4\theta+\cos^4\theta)
\end{aligned} \tag{13}$$

where [$Q$] is the reduced stiffness matrix and $\theta$ is ply angle.

### 2.3. Finite element analysis

Buckling analysis was performed using finite element analysis program. During the analyses, the effects of circular, triangular, square and elliptical cutouts are investigated. To understand the main effects, different parameters such as size, angle and orientation of cutouts are compared by keeping the cutout areas the same. Finite element analysis of composite lamina was performed using ANSYS 11.0 (Swanson Analysis System Inc., Houston, PA, USA).

Cutout orientations are given in Figure 2. $H$ (height) and $L$ (length) are taken as equal, and a total of five different plate sizes (100, 150, 200, 250 and 300 mm) were used in the analyses. The thickness of the plate is taken as 1.6 mm, and the number of the layers is taken as 8. During analyses, three different cutout areas are considered. For the triangular cutout, an equilateral triangle is used and one side is taken as 20, 30 and 40 mm for analyses; and for the other cutouts, areas are kept constant by using the suitable radius and side parameters. Also, five different fiber orientation angles (FOA; 0°, 15°, 30°, 45° and 60°) are used and four different cutout orientation angles (COA; 0°, 15°, 30° and 45°) are used in the analyses. A total of 1200 different finite element models were used in analyses.

Plates are meshed with quadratic composite shell elements (SHELL91) based on first-order shear deformation theory. SHELL91 [18] element geometry illustrated in Figure 3 can be used for layered applications to produce mesh structure. The element has six degrees of freedom at each node: translations in the nodal $x$, $y$ and $z$ directions and rotations about the nodal $x$-, $y$- and $z$-axes.

Because of the different cutout dimensions and angles, different models and mesh structures are prepared. Optimum mesh structures are shown in Figure 4. As can be seen in this figure, the model was meshed with quadrilateral elements for a good mesh generation. In addition, the mesh around the cutout is refined to get a better mesh structure because the close areas of the cutout were very critical for finite element solutions. Refining the mesh provides a sensitive solution. Also, the boundary conditions and loadings of the models are illustrated in Figure 4. The pre-buckled stress distribution was evaluated under 1 N/m uniform load and saved for the eigenvalue buckling solution. Then, the eigenvalue buckling load was determined. This procedure was carried out for all of the models.

## 3. Results and discussion

In this study, buckling loads were found by theoretical and numerical methods. To investigate finite element model

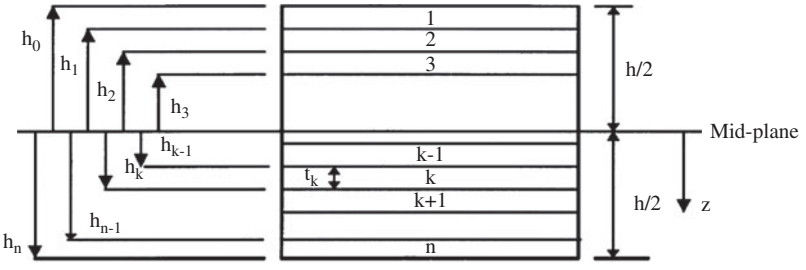


**Figure 1** Coordinate locations of plies in a laminate.

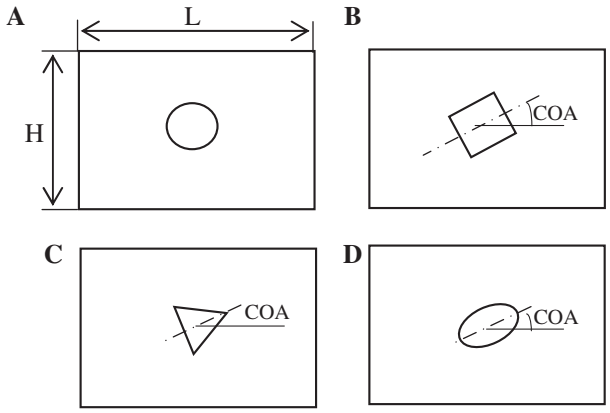


**Figure 2** Cutouts used in the analyses: (A) circular, (B) square, (C) triangular and (D) elliptical.

accuracy, firstly an un-perforated plate was analyzed for 0° fiber angle and 8 layers with 1.6 mm plate thickness. Using Eq. 8, theoretical buckling load of lamina was calculated. Also, for un-perforated plates, experiments were performed using Shimadzu AG-X series testing machine (Shimadzu Corporation, Kyoto, Japan). Obtained critical buckling loads are presented in Table 2 and comparisons are presented in Figure 5. The results are in close agreement with each other.

### 3.1. The effect of fiber orientation

The buckling analysis of composite lamina was performed for perforated plates. Change of buckling loads for circular, square, triangular and elliptical cutouts with respect to fiber orientation angle is shown in Figure 6 for 100 mm plate. It is seen that buckling load is minimum when the fiber angle used is 45°, and after this angle critical buckling load begins to increase. It can also be concluded that, up to fiber orientation angles of 45°, elliptical cutout has maximum critical buckling load, but after 45°, circular cutout has maximum value.

### 3.2. The effect of plate size

Change of critical buckling loads for 150-, 200-, 250- and 300-mm plate lengths are shown in Figure 7. Critical buckling load is minimum for all plate sizes when fiber angle is 45°. Buckling load decreases with increasing plate length, but buckling load behavior generally stays the same.

Change of critical buckling load with respect to plate size is given in Figure 8. Critical buckling load decreases when plate size is increased and curve of change is nearly the same for all types of cutouts.

### 3.3. The effect of cutout angle

The effects of cutout orientation angle on critical buckling load are given in Figure 9. As can be seen from Figures 6 and 7, when fiber orientation angle 0° is used, elliptical cutout gives the highest buckling load; whereas when fiber orientation angle 45° is used, circular cutout gives the highest buckling load. Therefore, when the effects of cutout orientation angle are analyzed, 0° and 45° fiber orientation angles (with respect to critical buckling load) are considered. In Figure 9A, elliptical cutout has the highest buckling load at all cutout angles (although there is numerical difference between angles) and in Figure 9B, circular cutout has the highest buckling load almost at all cutout angles (except 30°). Furthermore, to see the same effect on a different size of plate, in Figure 9C and D, changes of critical buckling load with respect to cutout angle are given for 150-mm plate size. Again, similar changes are observed in these two graphs.

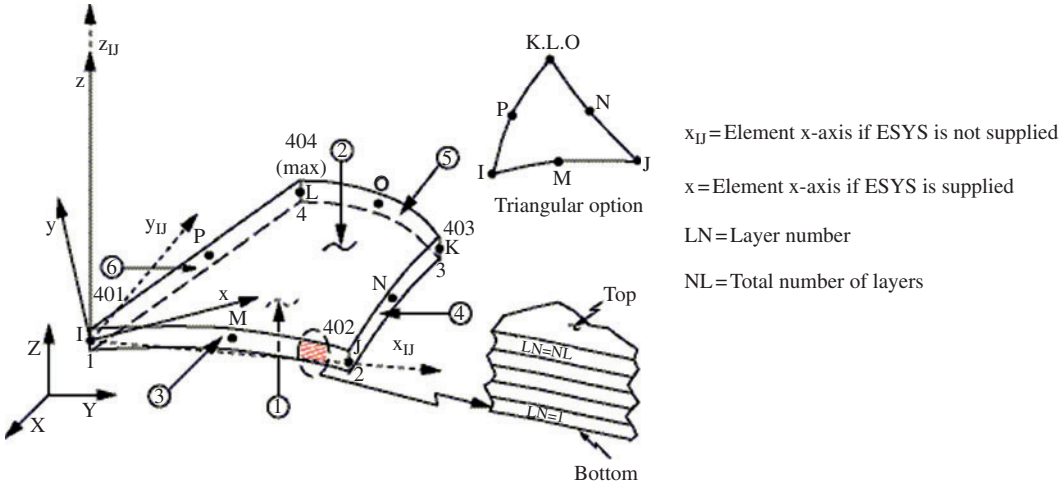


**Figure 3** SHELL91 geometry [18].

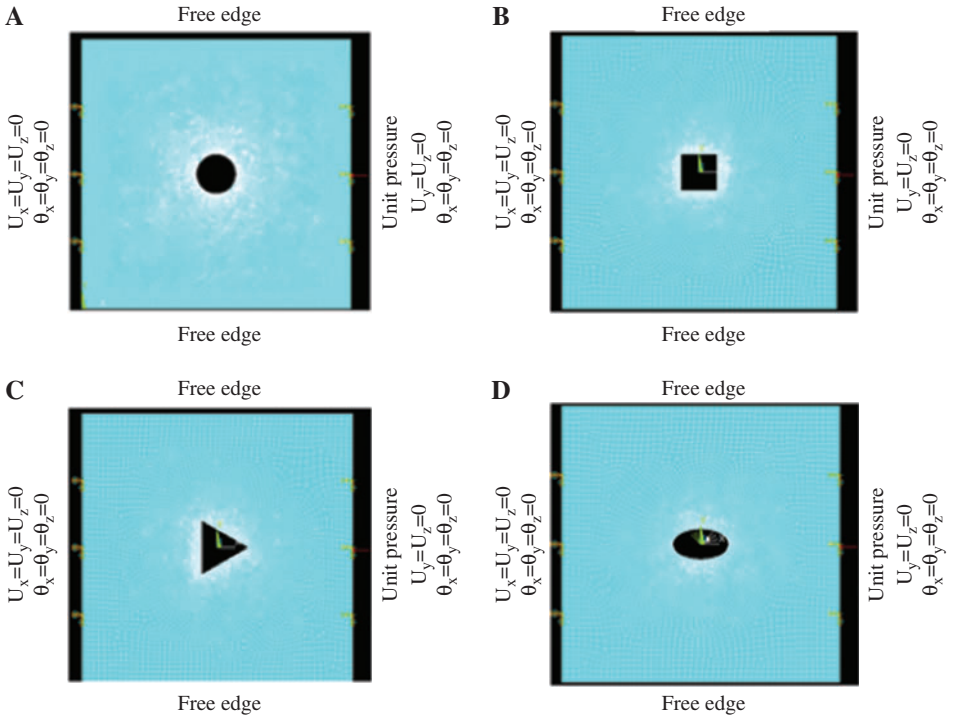


**Figure 4** Mesh and boundary conditions: (A) circular cutout, (B) square cutout, (C) triangular cutout and (D) elliptical cutout.

### 3.4. The effect of cutout area

Changes of critical buckling load with respect to cutout area are given in Figure 10. As seen in the figure, for all cutout types, critical buckling load decreases when cutout area is increased.

## 4. Conclusions

In this study, the effects of circular, square, triangular, and elliptical cutouts on the buckling behavior of laminated composite plates were investigated. Buckling analysis for perforated composite laminates was performed, and the effects of types, sizes and orientations of cutouts were investigated. Fiber orientation angle and size of plates were also investigated and the results can be summarized as:

- Fiber orientation angle and cutout sizes are the most important parameters on the critical buckling loads.
- The buckling loads of plates are decreased by increasing the fiber orientation angle. The most critical buckling load is fixed when fiber angle was used as 45°, and after this angle critical buckling load begins to increase.
- From 0° to 45° fiber orientation angle, elliptical cutout has the highest buckling load, but after 45° circular cutouts have the highest buckling load.
- The increase in COA causes very little decrease of buckling loads of plate. COA is less effective on buckling load.

**Table 2** Buckling load of 0° un-perforated glass-polyester composite plate.

| Plate size (mm) | $P_{cr}$ theoretical (N/mm) | $P_{cr}$ numerical (ANSYS) (N/mm) | $P_{cr}$ experimental (N/mm) |
|---|---|---|---|
| 100×100 | 42.94 | 43.44 | 40.82 |
| 150×150 | 19.13 | 19.42 | 18.26 |
| 200×200 | 10.82 | 10.94 | 10.38 |
| 250×250 | 6.87 | 7.014 | 6.68 |
| 300×300 | 4.79 | 4.873 | 4.67 |

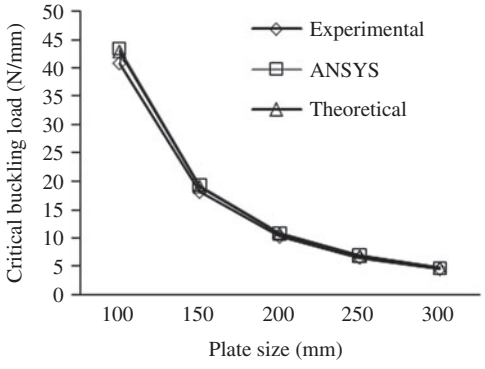


**Figure 5** Comparison of the experimental, ANSYS and theoretical results.

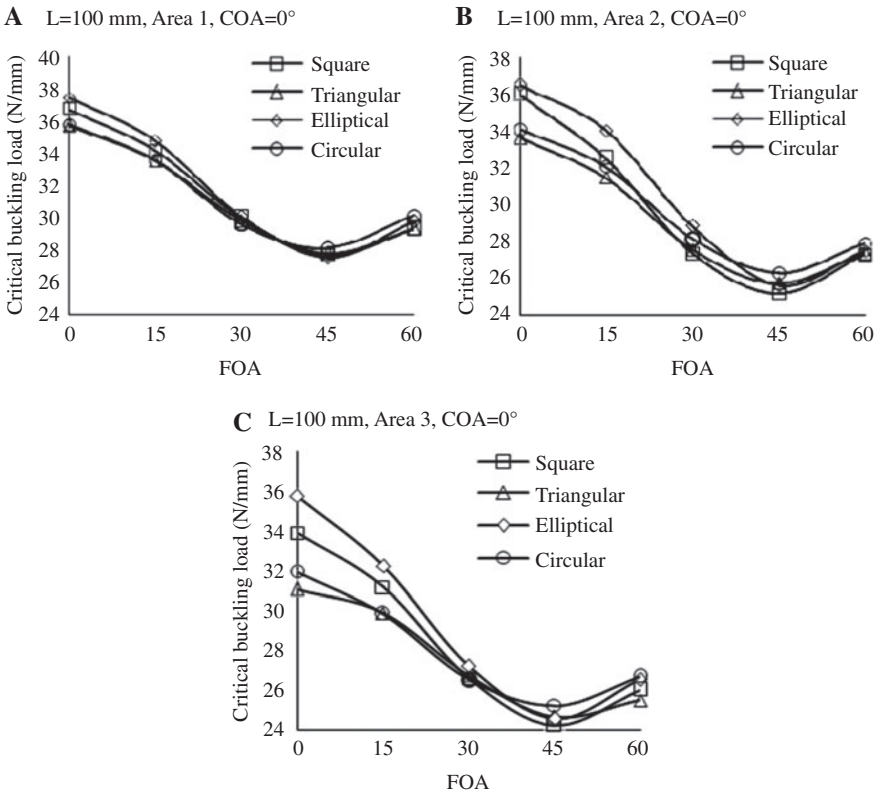


**Figure 6** Effects of FOA on buckling load for $L$=100 mm: (A) area 1, (B) area 2 and (C) area 3.

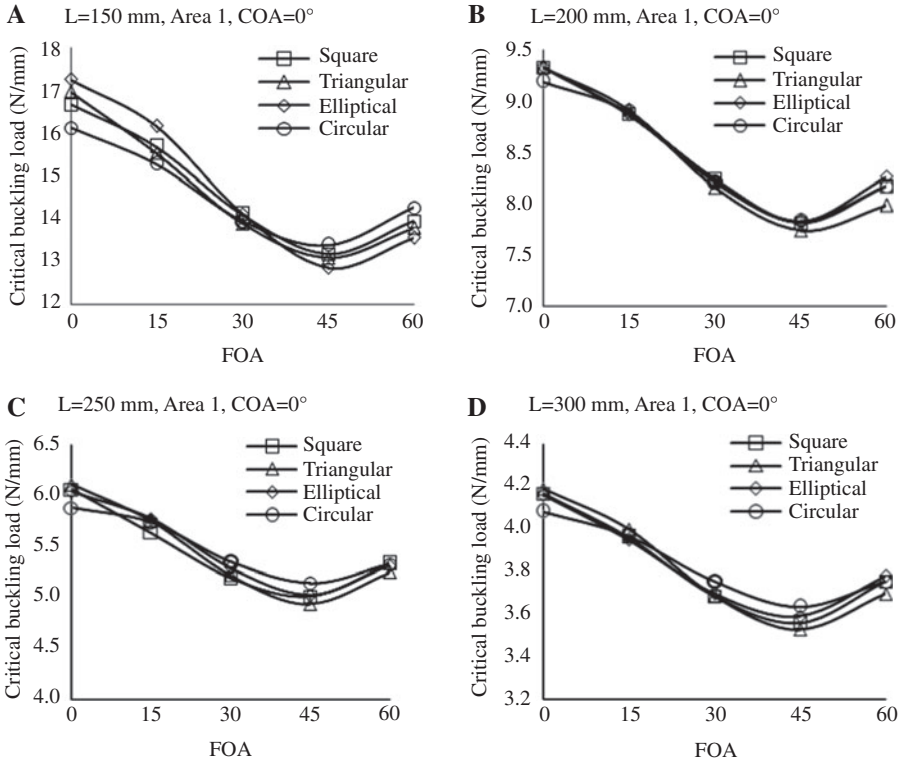


**Figure 7** The effects of FOA on buckling load of the composite plates for $L$ (A) 150 mm, (B) 200 mm, (C) 250 mm and (D) 300 mm.

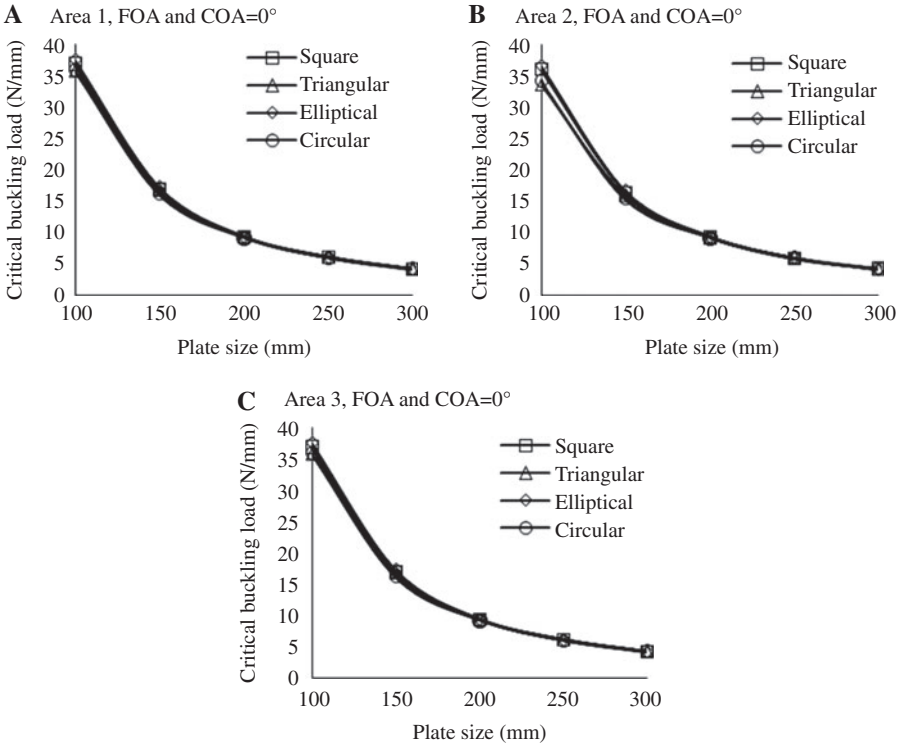


**Figure 8** The effects of plate size on buckling load of the composite plates, FOA and COA=0° and cutout area (A) 1, (B) 2, (C) 3 used.

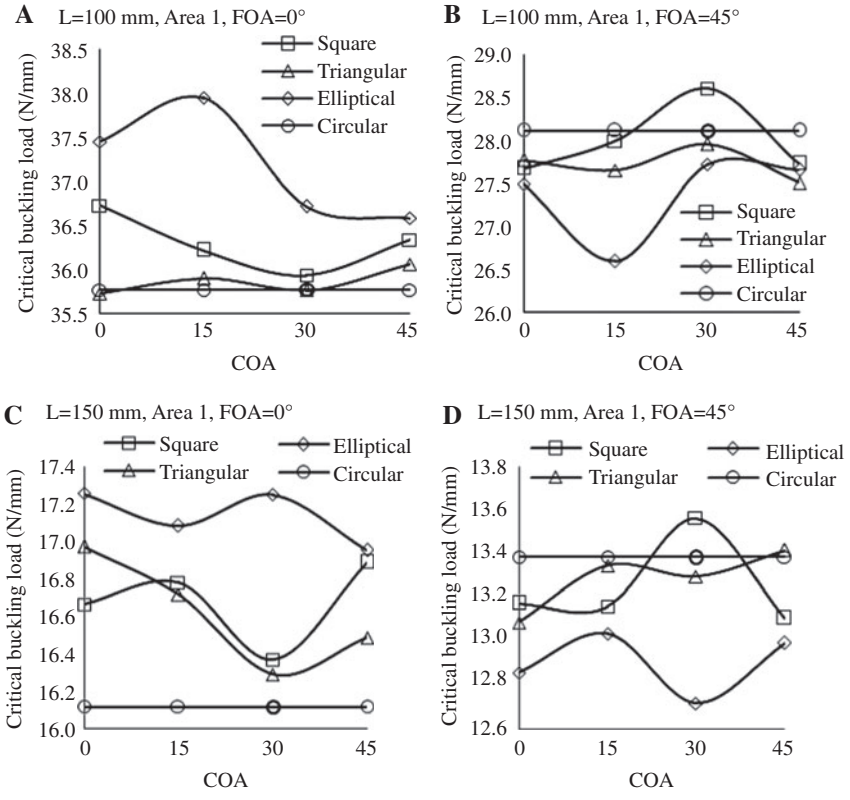


**Figure 9** Effects of COA on critical buckling load (A) FOA=0°, L=100 mm, (B) FOA=45°, L=100 mm, (C) FOA=0°, L=150 mm and (D) FOA=45°, L=150 mm.

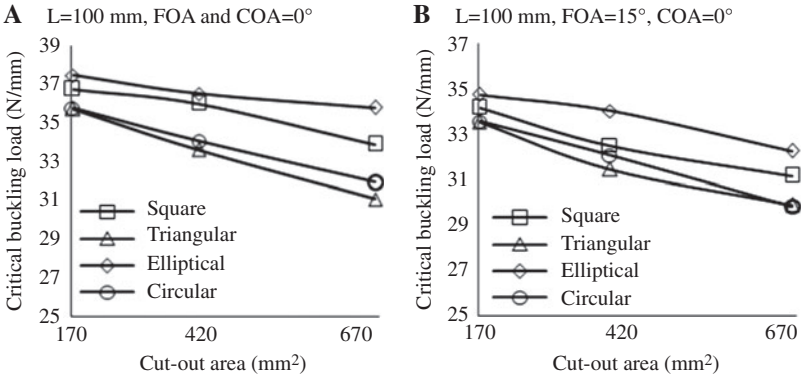


**Figure 10** The effect of COA on critical buckling load of the composite plates: (A) FOA=0°, L=100 mm; (B) FOA=15°, L=100 mm.

- Critical buckling load decreases when the size of the plate is increased.
- For all cutout types, critical buckling load decreases when cutout area is increased.

## References

[1] Kaw AK. *Mechanics of Composite Materials*, 2nd ed. Taylor & Francis, Inc.: London, 2006.
[2] Lin CC, Kuo CS. *Compos. Mater.* 1989, 23, 536–553.
[3] Nemeth MP. *AIAA* 1988, 26, 330–336.
[4] Britt VO. *AIAA J.* 1994, 32, 2293–2299.
[5] Lee HH, Hyer MW. *AIAA J.* 1993, 31, 1293–1298.
[6] Akbulut H, Sayman O. *J. Reinf. Plast. Comp.* 2001, 20, 1112–1124.
[7] Ghannadpour SAM, Najafi A, Mohammadi B. *Comp. Struct.* 2006, 75, 3–6.
[8] Baltacı A, Sarıkanat M, Yıldız H. *J. Reinf. Plast. Comp.* 2006, 25, 733–744.
[9] Yapıcı A, Sahin ÖS, Arıkan H. *J. Reinf. Plast. Comp.* 2005, 24, 1379.
[10] Baba BO, Baltacı A. *Appl. Compos. Mater.* 2007, 14, 265–276.
[11] Akbulut H, Ural T. *J. Thermoplast. Comp. Mater.* 2007, 20, 371–387.
[12] Yazıcı M. *J. Reinf. Plast. Comp.* 2008, 27, 1059–1070.
[13] Sahin M. *Experimental and Numerical Analyses of Laminated Composite Plates Subjected to Buckling Load. A Major Project Report for the Degree of Master in Mechanical Engineering*. Cumhuriyet University, 2008.
[14] Topal U, Uzman U. *Struct. Multidisc. Optim.* 2008, 35, 31–139.
[15] Qablan HA, Katkhuda H, Dwairi H. *Jordan J. Civil Eng.* 2009, 3, 184–195.
[16] Komur MA, Sen F, Atas A, Arslan N. *Adv. Eng. Software* 2010, 41, 161–164.
[17] Vinson JR, Sierakowski RL. *The Behavior of Structures Composed of Composite Materials*, 2nd ed., Kluwer Academic Publishers: London, 2004.
[18] *ANSYS Procedures. Engineering Analysis System Verification Manual, Vol. 1*. Swanson Analysis System Inc.: Houston, PA, USA, 1993.